Spodumene tailings for porcelain and structural materials: effect of temperature (1050-1200 ºC) on the sintering and properties

Patrick N. Lemougna[1*], Juho Yliniemi [1], Arnold Ismailov[2], Erkki Levanen[2], Pekka Tanskanen[3], Paivo Kinnunen,[1] Juha Roning [4], and Mirja Illikainen[1]

[1]Faculty of Technology, Fibre and Particle Engineering Unit, PO Box 4300, 90014 University of Oulu, Finland.
[2]Materials Science, Faculty of Engineering and Natural Sciences, Tampere University, P.O. Box 599, FI-33101 Tampere, Finland.
[3]Process Metallurgy Research Unit, University of Oulu, P.O. Box 4300, 90014 Oulu, Finland.
[4]InfoTech Oulu, Faculty of Information Technology and Electrical Engineering, Biomimetics and Intelligent Systems Group (BISG), University of Oulu, Oulu, Finland.

*Corresponding author: Patrick.LemougnaNinla@oulu.fi; lemougna@yahoo.fr

Abstract:

The use of industrial by-products as substitute to conventional natural resources in ceramic production is of interest from an environment preservation and solid wastes management. This paper deals with the recycling of tailings from spodumene concentration during lithium production (Quartz Feldspar Sand; QFS), for the production of porcelain and structural materials. The QFS obtained from spodumene processing consisted mainly of quartz, albite, microcline with traces of muscovite. Mixtures of QFS and standard porcelain ingredients were sintered at 1050-1200 °C at 50 °C intervals and their properties were compared with a conventional porcelain composition prepared under the same conditions. Phase composition was assessed by XRD analysis using Rietveld refinement. Tests such as water absorption, apparent density, sintering shrinkage, compressive and flexural strength were used for physical comparison. The results showed that higher densification was achieved at 1200 °C, with a drastic reduction of water absorption below 1%. A compressive strength of 40 MPa was obtained at 1050 °C in the composition made of 50 wt% QFS and 50 wt% kaolin, increasing to 85 MPa at 1100°C. The strength increase was attributed to better glassy phase formation and mullite growth. The QFS was found to contain no hazardous elements and showed promising sintering results, indicating its high suitability to substitute conventional resources in the production of ceramic materials.

Key words: Mine tailings; Quartz; Feldspars; Porcelain; Structural applications

1. Introduction

The concept of zero waste approach is gaining more and more interest due to the continuous increase in the amount of industrial by-products generated annually, and the concomitant shortage of some non-renewable natural resources used as feedstock materials for many industries (Ahmed Dabwan and Rubaiah Bt. Che Jaafar, 2018; Fernandes and Ferreira, 2007; Guan et al., 2018; Lassinantti Gualtieri et al., 2018; Saeli et al., 2019). Among these industrial by-products, lithium mine tailings are expected to dramatically increase in the coming years, due to increasing demand in lithium in the global market (Martin et al., 2017; Swiss Resource Capital AG, 2017; Tian et al., 2018). The global production of lithium estimated as lithium carbonate equivalent was about 175,000 tons in 2015 according to Swiss Resource Capital AG 2017. This production is largely driven by the rechargeable battery sector and is expected to reach 650,000 tons in 2025 and 1,000,000 tons by 2029 (Swiss Resource Capital AG, 2017).

Commercial lithium is derived from brine deposits or hard rock spodumene deposits (Meshram et al., 2014; Swain, 2017; Swiss Resource Capital AG, 2017). Due to the relatively low lithium content of about 6-7.5% LiO_2 in natural spodumene ($LiAl(SiO_3)_2$,) (Aylmore et al., 2018), the production of lithium from spodumene ore generates high volume of industrial by-products. For instance, according to the definitive feasibility study report on lithium production from spodumene ore of Keliber company, from an input of 600,000 tons/year of spodumene ore, about 11,000 tons of lithium carbonate will be produced, the balance being mainly rock and mine wastes, of which 350,000 tons are spodumene tailings (Keliber, 2018). Therefore, it is obvious that the beneficiation of these tailings is important to mitigate environmental impact and possibly lower the production cost. From their geological origin, spodumene is found in nature in pegmatite deposits, which comprises quartz, feldspars and micas as gangue minerals (Aylmore et al., 2018; Keliber, 2018; Wang et al., 2018). Accordingly, these minerals will be present in flotation tailings from spodumene concentration and a search for their beneficiation agrees with the concept of zero waste and the sustainable reuse of resource (Burlakovs et al., 2018; Esmaeilian et al., 2018; Karhu et al., 2018;

Veleva et al., 2017). Furthermore, concerns on depletion of feldspar deposits have raised interest for an efficient use of feldspar minerals (Zhang et al., 2018).

Natural feldspars are valuable raw materials for manufacturing of porcelains (Danezan et al., 2018; Sokolář et al., 2017). Porcelain belongs to ceramics and are attractive materials for their outstanding physical and chemical properties, which allow them to be used in a wide range of applications including household, aeronautic, energy, optics or biomedical domains (Carty and Senapati, n.d.; Danezan et al., 2018; Lerdprom et al., 2016; Soldati et al., 2018). Porcelains are typically made of kaolin clay, feldspar and quartz, usually in the proportion of about 50:25:25 wt% (Owoeye et al., 2018; Sokolář et al., 2017). Of these, clay is acting as plastic component, silica as filler and feldspars as fluxing agents, and the desired properties are defined or optimized by an interplay between raw materials, processing and firing conditions (Danezan et al., 2018; Güngör and Ay, 2018; Owoeye et al., 2018).

Demand for ceramic materials is increasing on daily basis (Owoeye et al., 2018), and the possible use of mine tailings in the production of ceramics is also complying with the concept of circular economy, an approach of economic growth that is in line with sustainability, environmental preservation and economic development (Korhonen et al., 2018; Winans et al., 2017).

The aim of this study was to investigate the potential of valorisation of quartz feldspar sand rich tailings (QFS) from lithium production for the development of structural and porcelain materials. A commercial kaolin was used and combined with QFS and quartz in the defined ratios. The mixtures were tested by heating to 1050, 1100, 1150 and 1200 ºC. The obtained materials were characterized by X-ray diffraction, thermogravimetry analysis, scanning electron microscopy, dilatometry analysis, density and water absorption. These properties were compared with a standard porcelain composition prepared under the same conditions using a commercial kaolin, a commercial feldspar and quartz.

2. Experimental

2.1. Materials

The QFS used in this study was from spodumene processing during pilot production of lithium hydroxide by Keliber Oy, Finland. A commercial kaolin, quartz and feldspar were purchased for the study. The chemical composition of the starting materials is presented in Table 1.

Table 1. Chemical composition of QFS, kaolin and commercial feldspar (wt%)

	SiO_2	Al_2O_3	Fe_2O_3	CaO	MgO	Na_2O	K_2O	TiO_2	P_2O_5	MnO	LOI
QFS	77.5	13.5	0.2	0.3	0.0	4.8	3.3	0.0	0.1	0.0	0.0
Kaolin	53.2	36.8	1.2	0.1	0.3	0.2	2.5	0.1	0.2	0.0	10.9
Commercial feldspar	70.8	17.0	0.1	1.3	0.1	6.6	3.9	0.1	0.0	0.0	0.1
Quartz	99.3	0.3	0.2	0.0	0.0	0.0	0.1	0.0	0.0	0.0	0.0

The as received QFS with d50 of 171 µm was ground for six hours in a ball mill to achieve a d50 below 10 µm. The particle size information of the QFS and the different porcelain compositions (see Table 2) is presented in Figure 1.

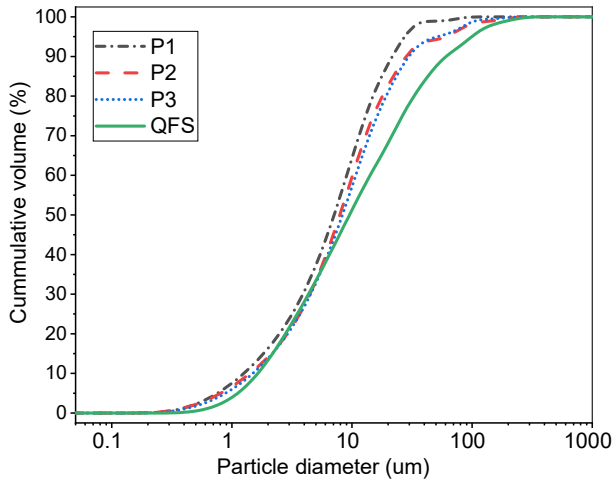

Figure 1: Particle size distribution of QFS and referred compositions

2.2. Specimens preparation

Based on the phase composition of QFS (44% albite, 32% quartz, 11% microcline, 6 % muscovite and 7% amorphous +unknown) determined in preliminary investigation, specimens from QFS and kaolin were formulated to be close to the reference porcelain composition of 50 wt% kaolinite, 25 wt% feldspar and 25 wt% quartz. An appropriate amount of water was added to the mixture to obtain a plastic paste which was shaped in rectangular 320 mm^3 alloy molds (80×20×20 mm). Based on the promising results on the mechanical properties obtained on the porcelain composition at 1050 °C, the formulations S1 and S2 containing 80 and 90 wt% QFS respectively, which are not porcelain compositions, were also prepared to assess their suitability for structural applications such as building bricks. The heating rate was 5 °C per min, and the dwell time was 2 hours at the maximum temperature. The details on the mixture proportioning are presented in Table 2.

Table 2: Mixture proportioning

Ref	QFS (g)	Quartz (g)	Kaolin (g)	Commercial feldspar (g)	Water	Sintering temperature
P1 (QFS50K50)	50	-	50	-	38	1050, 1100,1150 1200°C
P2(QFS41Q9K50)	41	9	50	-	38	
P3(Q25K50F25)	0	25	50	25	38	
S1(QFS80K20)	80	-	20	-	30	1050°C
S2(QFS90K10)	90	-	10	-	25	

2.3. Characterization methods

2.3.1. XRD analyses

The starting materials and the prepared ceramics were ground in a RETSCH 200 vibratory disc mill:1000tr/min for 3 min. The powdered materials were examined by X-ray diffraction using a Rigaku Smartlab diffractometer, with a Cu K-beta radiation, step width of 0.02º, scan speed 4.0628 º/min, 2θ range of 5–80º, operated at 135 mA and 40 kV. The quantification of the crystalline phases was done using the Rietveld refinement method and 10 wt% rutile (TiO_2) as internal standard.

2.3.2. SEM/EDX analysis

The QFS and prepared ceramics were cast in epoxy resin for polishing. The samples were then coated with carbon and analysed using Scanning Electron Microscopy (SEM) and Energy Dispersive X-ray Spectroscopy (EDX) (Zeiss Ultra Plus). Analyses were performed with a backscatter electron detector with 15 kV acceleration voltage and the working distance was about 8.2 mm.

2.3.3. Compressive and flexural strength, water absorption and apparent density

The determination of the three-point flexural strength was performed using a Zwick testing machine with a maximum load of 100 kN and a loading rate of 0.05 kN/s. The supports span was 40 mm. The flexural strength (δ) was determined using the equation below:

$$\delta = 3FL/2bd^2$$

Where: δ is flexural strength in N/mm^2; F is maximum load in N; L is supports distance in mm; b is width of the tested beam in mm and d is height of the tested beam in mm.

The compressive strength was also performed using the Zwick testing machine, with a loading rate of 2.4 kN/s. For each composition, at least three replicates specimens were tested, and the average

was regarded as the representative value of the strength. The error bar in Figure 8 indicates the standard deviation between specimens.

The water absorption was determined by immersing the samples in deionized water for 24 hours and the apparent density was determined using the Archimedes' principle according to SFS-EN 1936 standard.

2.3.4. Thermogravimetric and dilatometry analysis

Thermogravimetric analysis (TG) was performed with a simultaneous TG/DSC measurement in air, using a NETZSCH STA 449F3 TG/DSC instrument at a constant heating rate of 5 °C/min. The samples were heated from room temperature to 1200 °C.

The samples for dilatometry analysis were molded and cut to 8×8×10 mm and the determinations were performed on a NETZSCH DIL 402 Expedis dilatometer. Prepared samples were heated in two cycles: Firstly to 1200 ºC at 5 ºC/ per min, 2 hours dwell time, and secondly at 1200 ºC, heating rate 5 ºC/ per min and 1-hour dwell time. The heating chamber was open ended, where a constant flow of nitrogen (40 ml/min) was used as the purge gas to prevent unwanted gaseous/evaporated matter getting into the measurement chamber, which was separate from the heating chamber where the sample was put.

3. Results and discussion

3.1. Phase composition

The XRD spectra of the QFS, kaolin, quartz and commercial feldspar used for the preparation of the porcelain compositions is presented in Figure 2.

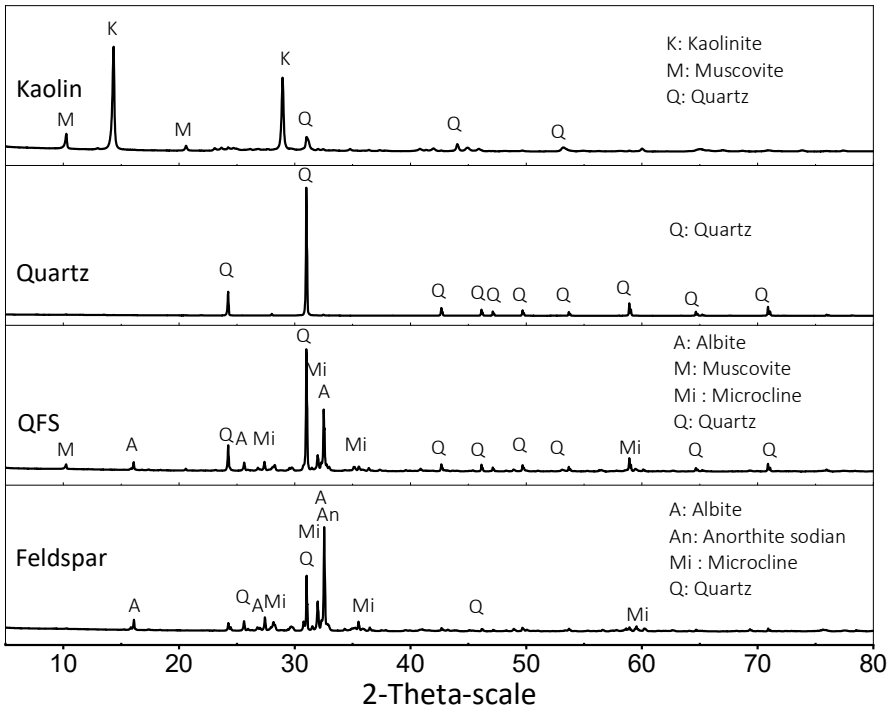

Figure 2: XRD spectra of kaolin, quartz, QFS and commercial feldspar

Kaolin contained mainly kaolinite ($Al_2Si_2O_5(OH)_4$, pdf. 04-013-2815), with trace of muscovite ($K_{0.8}$ $Na_{0.2}$ $Fe_{0.05}$ $Al_{2.95}$ $Si_{3.1}O_{10}(OH)_2$, pdf. 04-012-1906) and quartz (SiO_2, pdf. 04-014-7568). The QFS was mainly composed of albite ($Na_{0.98}Ca0.02Al_{1.02}Si_{2.98}O_8$, Pdf. 04-017-1022), microcline ($KAlSi_3O_8$, pdf 04-008-1783), quartz (SiO_2, pdf. 04-014-7568) and trace of muscovite ($K_{0.8}Na_{0.2}Fe_{0.05}Al_{2.95}Si_{3.1}O_{10}(OH)_2$, pdf. 04-012-1906). The commercial felspar contained albite ($Na_{0.98}Ca0.02Al_{1.02}Si_{2.98}O_8$, pdf. 04-017-1022), microcline ($KAlSi_3O_8$, pdf 04-008-1783), quartz (SiO_2, pdf. 04-014-7568), and trace of sodian anorthite ($Na_{0.30}Ca_{0.63}Al_{1.63}Si_{2.38}O_8$, pdf. 04-011-6816), meanwhile the quartz presented only crystalline reflection of quartz mineral. The mineralogical composition of QFS was in agreement with reported information for spodumene ores (Aylmore et al., 2018; Kuang et al., 2018). It can also be noted that QFS presented some similarity

in the mineralogical composition with the commercial feldspar, suggesting it could replace feldspars in some applications.

The XRD spectra of the sintered P1 (QFS50K50), P2 (QFS41Q9K50) and P3 (Q25K50F25) porcelain compositions at 1050 and 1200 °C are presented in Figure 3.

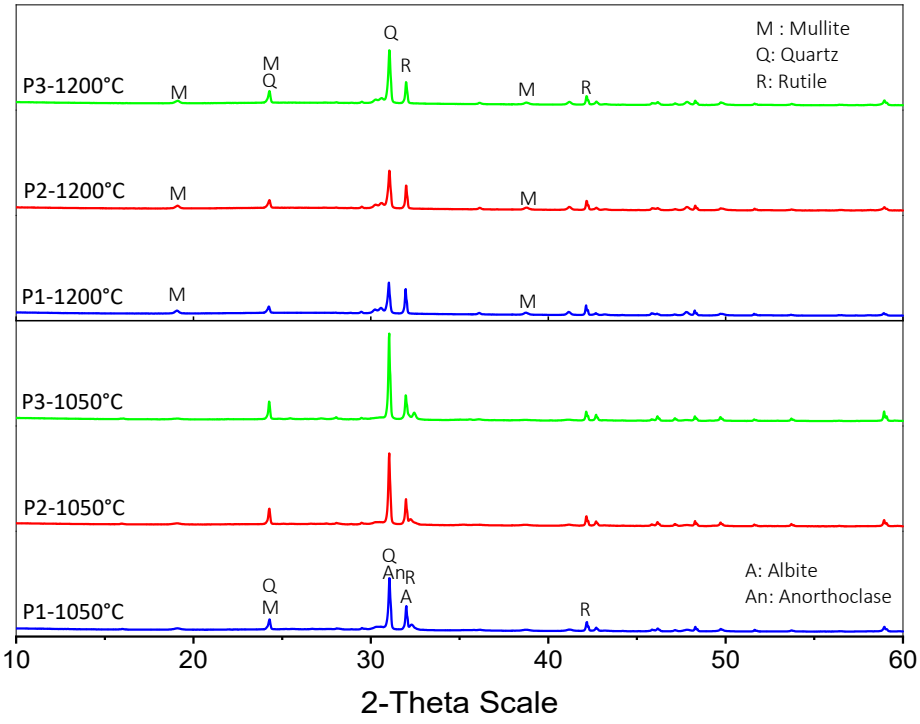

Figure 3: XRD spectra of compositions P1 (QFS50K50), P2 (QFS41Q9K50) and P3 (Q25K50F25), sintered at 1050 and 1250 ºC

A reduction of crystalline reflections was observed when the material was sintered from 1050 to 1200ºC and was attributed to the increase in the glassy (amorphous) phase content in the samples. At 1050 °C, the crystalline reflections of porcelain like compositions were mainly made of albite, mullite and quartz, while at 1200 °C, only mullite and quartz remained as crystalline phases. These observations agree with reported results on porcelain like compositions (Danezan et al., 2018; Gouvêa et al., 2015; Lerdprom et al., 2016; Lima et al., 2018). During the sintering of porcelain compositions, kaolinite first decomposes to an amorphous phase, then to mullite around 900 °C, the formation of the latter gradually increasing till 1100 °C before remaining stable between 1100 and 1200 °C (Güngör and Ay, 2018; Zanelli et al., 2003). The feldspars and quartz remain stable till about 900 °C, temperature at which their proportions start to decrease with the increase in melting

phase, the complete melting of feldspars occurring above 1150 °C (Zanelli et al., 2003). The lower crystalline reflections of P1 observed in Figure 3 was attributed to a higher proportion of the glassy phase.

The quantitative phase analysis of compositions P1, P2 and P3 at 1050 and 1200 °C determined using the Rietveld refinement method is presented in Figure 4.

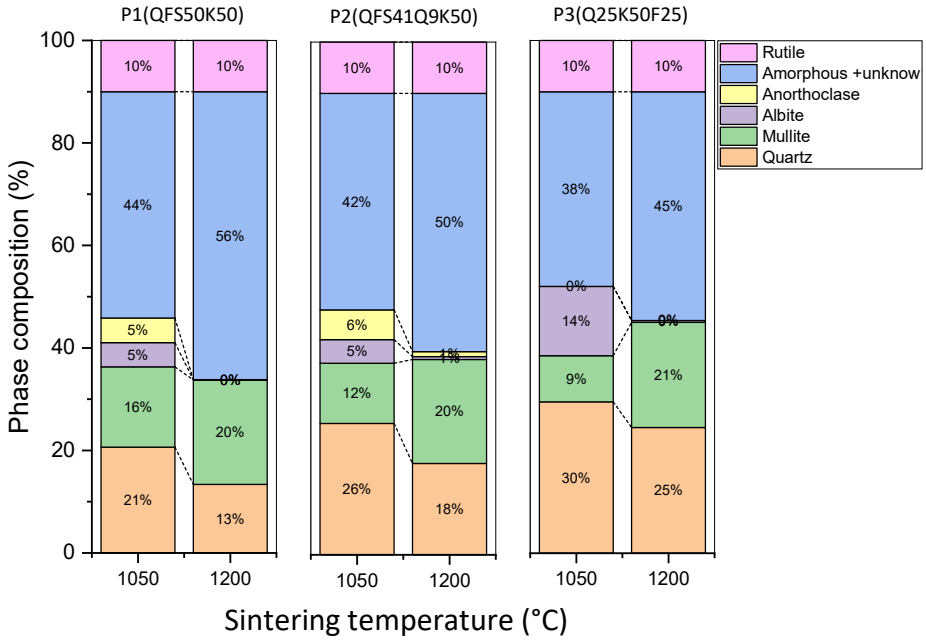

Figure 4: Phase composition of referred compositions at indicated temperatures

The quartz and albite proportion were found to reduce in all the samples with an increase in the sintering temperature, at variance to mullite and amorphous content. It was observed that albite had completely reacted while a higher proportion of mullite (around 20%) was observed at 1200 °C for all the compositions (Figure 4). However, at 1050 °C, specimen P1 presented the highest proportion of mullite (about 16%), as result of a better sintering reaction of this composition at lower temperature. In the three-axial composition of porcelain material (clay-quartz-feldspars), feldspars are acting as fluxing agent during the sintering and favour the formation of liquid phase (Owoeye et al., 2018; Sokolář et al., 2017). From the information presented in Figure 4, it could be deduced that

QFS contributed well for the formation of the glassy phase, suggesting its suitability in the replacement of commercial feldspars in ceramic formulations.

3.2. Microstructural analysis

Microstructural analysis was performed on QFS and polished sections of specimens treated at 1050 and 1200 °C. The QFS particles were found to be composed of separate mineral particles of albite, microcline and quartz (Figure 5).

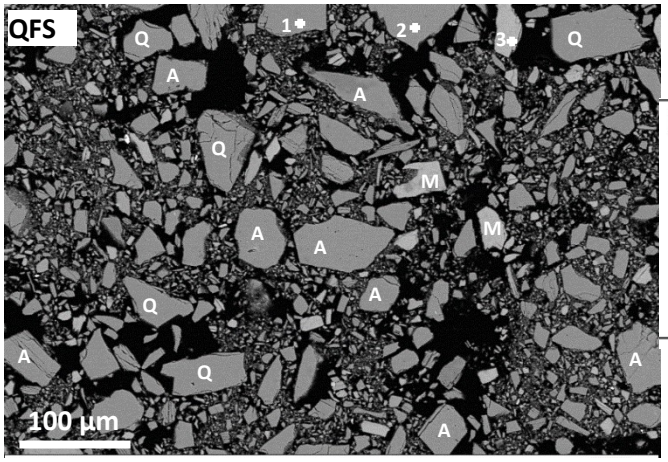

Element (Wt%)	1:Quartz (Q)	2: Albite (A)	3: Microcline (M)
O	48.44	44.12	41.65
Si	51.56	35.42	32.97
Al	-	11.52	10.68
Na	-	8.95	0.43
K	-	-	14.27

Figure 5: SEM of QFS powder

Quartz contains about 46.74 wt% Si and 53.26 wt% O. Albite contains about 8.30 wt% Na, 0.76 wt% Ca, 10.77 wt% Al, 31.50 wt% Si and 48.66 wt% O. Microcline contains about 14.05 wt% K, 9.69 wt% Al, 30.27 wt% Si and 45.99 wt% O. Considering this information and that obtained from XRD analysis, points 1, 2 and 3 were respectively ascribed to quartz, albite and microcline (Figure 5).

Polished sections of P1 and P3 treated at 1050 and 1200 °C are presented in Figure 6.

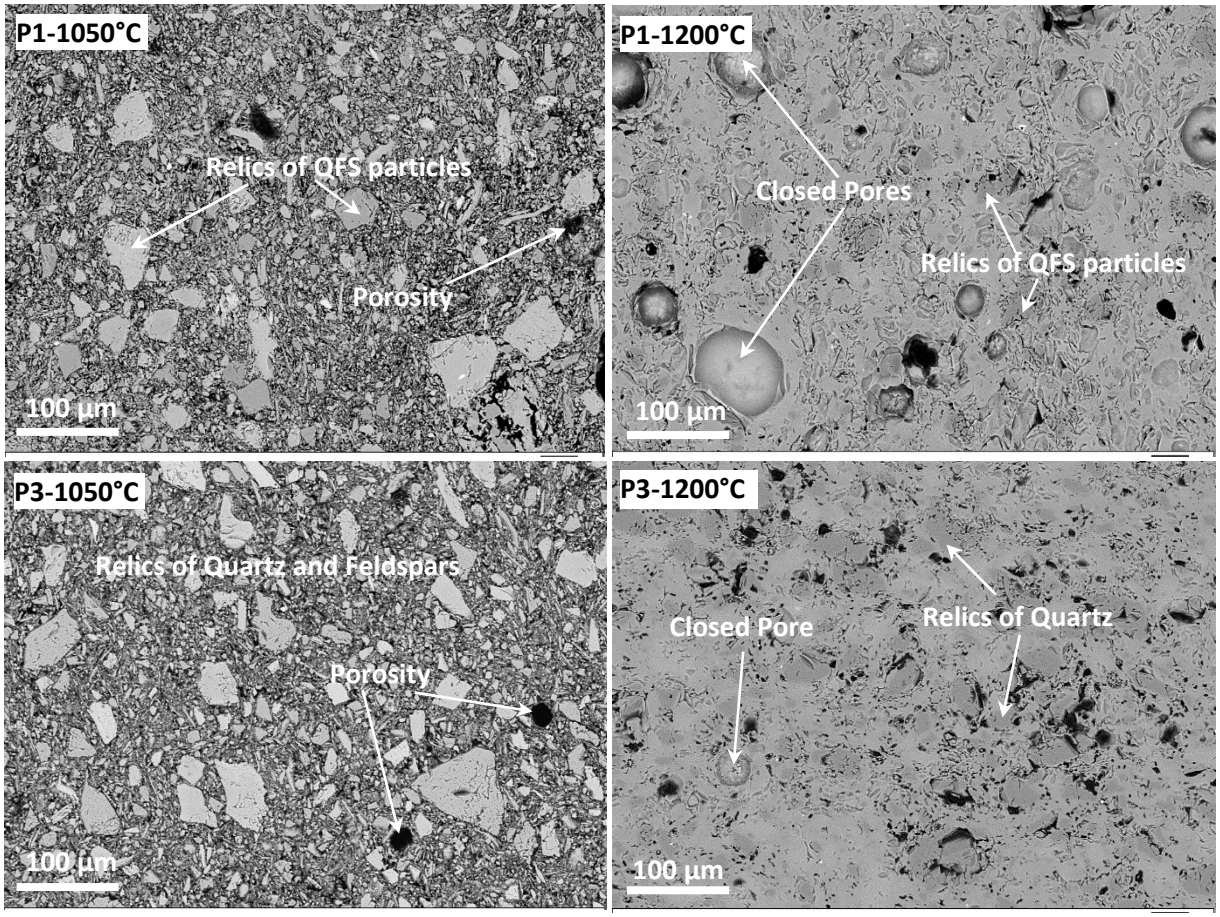

Figure 6: SEM images of P1 (QFS50K50) and P3 (Q25K50F25) at 1050 and 1200 °C

For the samples treated at 1050°C, relic of quartz and feldspar particles similar to the starting materials with quite well-defined boundaries were clearly visible as result of minor solid-state sintering reactions. No clear evidence of melting was observed compared to specimens treated at 1200 °C which presented a compact and dense microstructure because of well proceeded sintering via partial melting of the materials. P1 also presented less quartz relics than P3, in agreement with XRD analysis.

At higher magnification (Figure 7), samples P1 and P2 were well densified, presenting similar microstructural features with the reference porcelain composition (P3). The microstructure images showed relic of quartz particles. Some black shade features ascribed to porosity were also observed.

Grey round shaped smooth pores, some containing tiny crystals, were from gas bubbles in liquid state. Black and more ‘‘angular’’ pores were mainly because of loosing of particles during polishing. This is in agreement with reported studies on the microstructure of porcelain materials which generally consists of mullite, undissolved quartz, glassy phase, and sometime residual feldspar and porosity (Güngör and Ay, 2018; Owoeye et al., 2018).

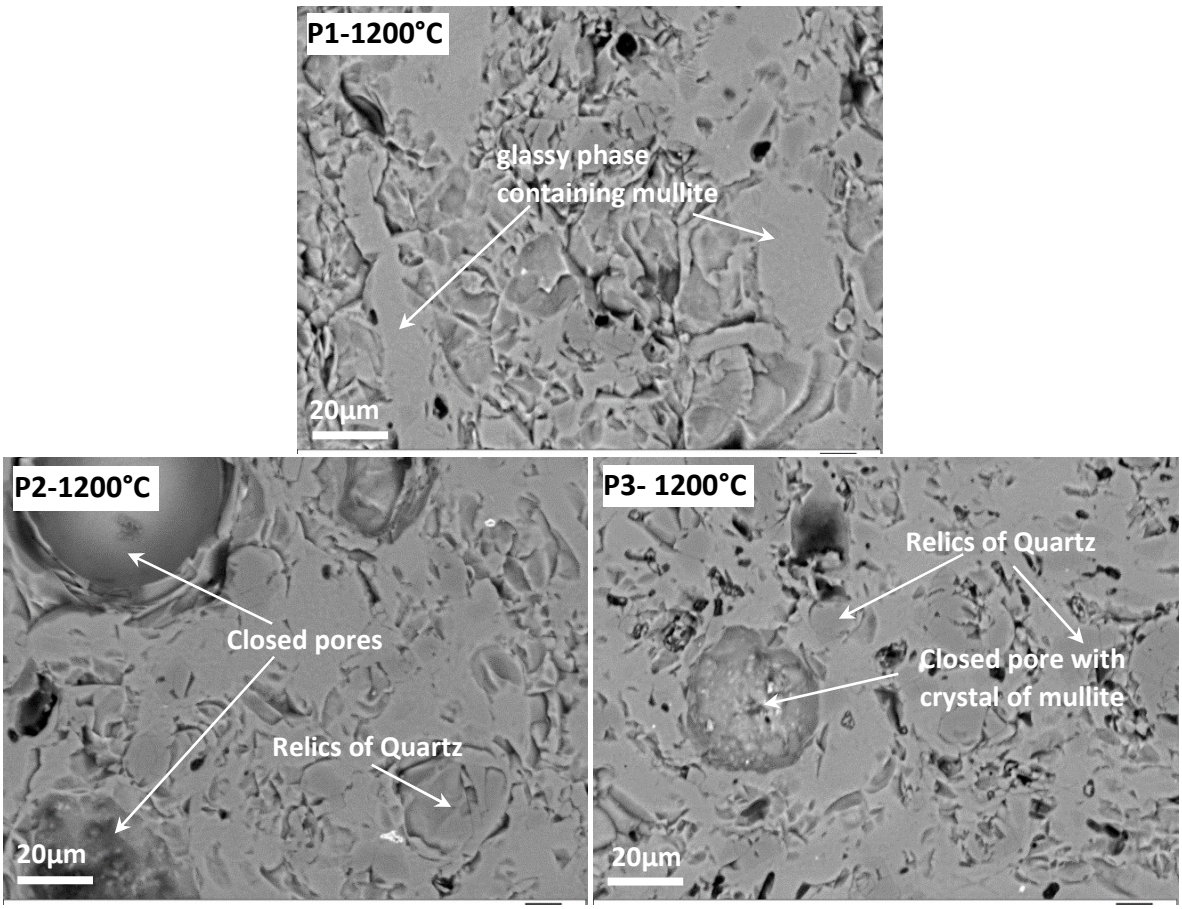

Figure 7: SEM images of P1(QFS50K50), P2(QFS41Q9K50) and P3(Q25K50F25) at 1200 °C

The presence of the relics of starting materials in porcelain formulation is linked to their initial particle size, their chemical and mineralogical composition as well as the heating program. The finer the particle size, the better the dissolution which remain low below 1200 °C (Güngör and Ay, 2018). This means better dissolution may have been observed if the heating temperature was raised above 1200 °C or the particle size of the materials reduced. Densification, resulting from the formation of viscous liquid can start at different temperatures depending on the mineralogical and

chemical composition as well as the particle size of starting materials. As the temperature increases, some eutectic melts resulting from the reaction of feldspar particles and SiO_2 from the initial kaolin can start to form at 990 °C, and will progressively fill the pores in the microstructure (Güngör and Ay, 2018; Sokolář et al., 2017). The microstructure of P1, P2 and the referred porcelain composition (P3) were almost similar, confirming the possible suitability of QFS for a use as raw material for porcelain compositions.

3.3. Compressive and flexural strength

The compressive strength of the specimens is presented in Figure 8.

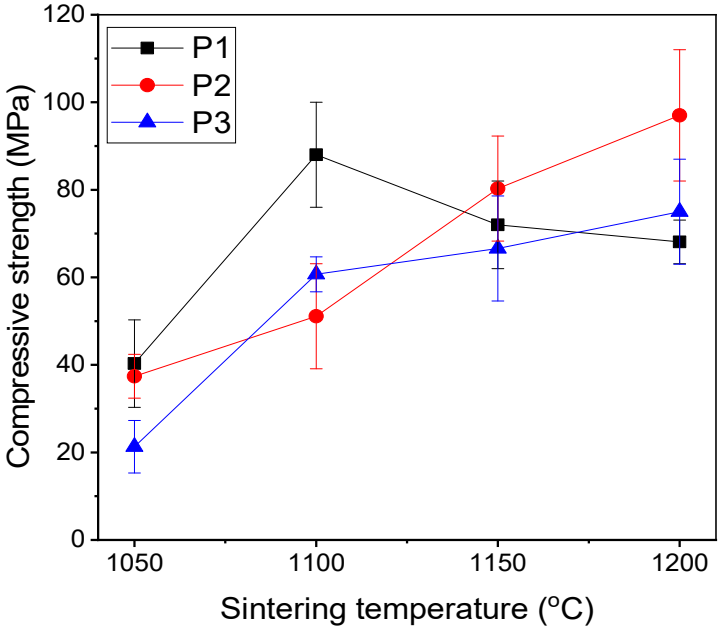

Figure 8: Effect of sintering temperature on the compressive strength of P1 (QFS50K50), P2(QFS41Q9K50) and P3 (Q25K50F25)

The compressive strength was found to increase with the investigated sintering temperature range for compositions P2 and P3. Composition P2 presented a compressive strength of about 40 and 90 MPa at 1050 and 1200 °C respectively, while composition P3, the reference composition, presented a compressive strength of about 20 and 75 MPa at 1050 and 1200 °C respectively. The trend of strength increase with the sintering temperature was not observed for composition P1 which presented its highest compressive strength (85 MPa) at 1100°C. The compressive strength of P1 then slightly decreased with the increase of the sintering temperature to about 70 MPa at 1200°C.

The fact that P1 presented higher compressive strength at lower temperature indicates higher generation of glassy phase at this temperature in comparison to other compositions. Furthermore, one would expect higher strength at lower temperature with increased amounts of QFS. The composition P1 presented 40 MPa compressive strength at 1050°C, temperature belonging to the conventional temperature range for the production of conventional structural ceramics (Boltakova et al., 2017; Dalkılıç and Nabikoğlu, 2017; Kulkarni et al., 2019). The 40 MPa strength developed at this temperature also meet the requirement of most building materials including masonry bricks, fired bricks and paving bricks subjected to light traffic (Al-Fakih et al., 2019; Kizinievič et al., 2018; Lemougna et al., 2011; Murmu and Patel, 2018; Taurino et al., 2017; Weishi et al., 2018), suggesting QFS as suitable candidate for the development of structural ceramics, with possible admixture of clays.

The flexural strength of the prepared materials at indicated temperatures is presented in Figure 9.

In this Figure, it is observed that the maximum flexural strength of the three compositions is about 30 MPa. The maximum value of flexural strength was below 35 MPa, the value usually used as reference for porcelain compositions (Martín-Márquez et al., 2008). However, these values were comparable to some reported values of flexural strength of porcelain stoneware treated at 1200-1260 °C (Martín-Márquez et al., 2010). The lower value of the flexural strength may be attributed to the absence of high pressing operation during the shaping phase. It is noted that the strength evolution from 1050 °C to 1200 °C is not the same for the three compositions. The reference porcelain composition presented a gradual increase of the flexural strength when the temperature increased from 1050°C to 1200°C meanwhile the optimum flexural strength of P1 and P2, around 30 MPa, were obtained at 1100 and 1150 °C, respectively.

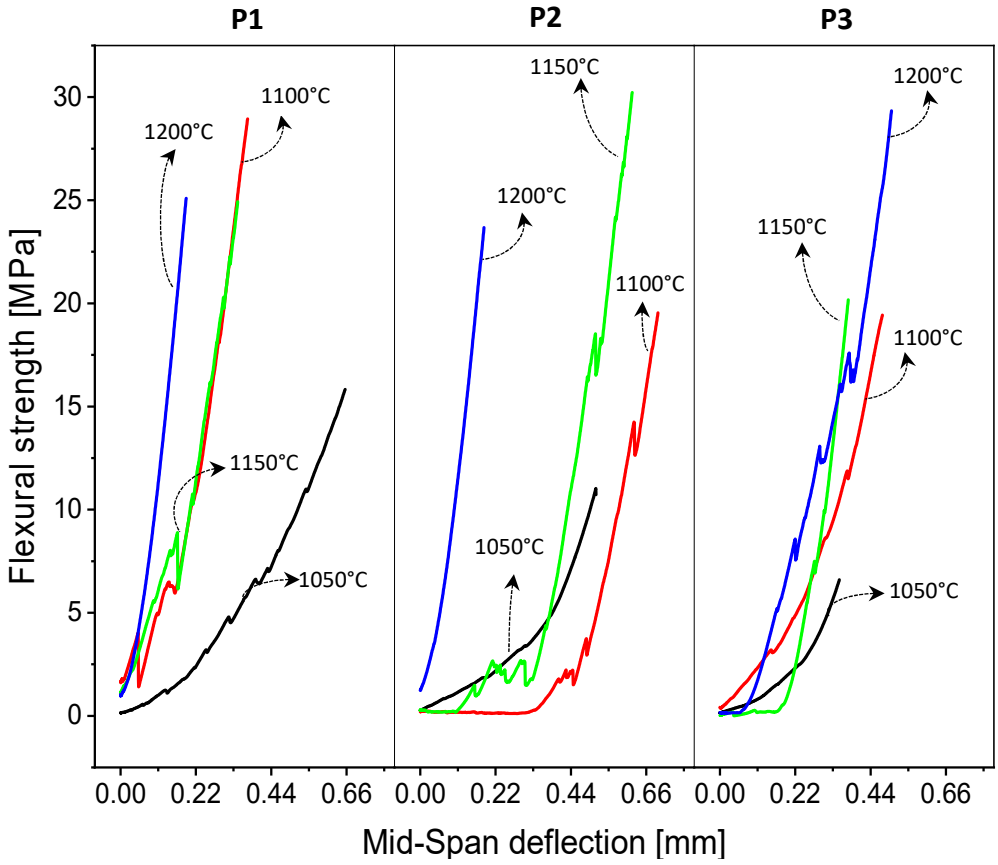

Figure 9: Effect of sintering temperature on the flexural strength of P1 (QFS50K50), P2 (QFS41Q9K50) and P3 (Q25K50F25)

The flexural strength of porcelain composition is an important property, which is related to the starting material composition and the processing conditions (Kitouni and Harabi, 2011; Martín-Márquez et al., 2010; Owoeye et al., 2018). It is suggested that the amount and particle size distribution of quartz grains significantly affect the mechanical strength of porcelain bodies. Indeed, some internal stresses due to difference in thermal linear expansion coefficients between quartz and the glassy phase, and alpha to beta quartz inversion around 573 °C negatively affect the strength. On the other hand, quartz is taking part in the formation of the crystalline mullite phase and glassy phase which are responsible of the development of mechanical strength (Kitouni and Harabi, 2011; Martín-Márquez et al., 2008). Figure 9 showed that substitution of 9 wt% QFS with quartz

presented some positive effect on strength at 1150 °C. The optimal effect of quartz on strength can then be achieved by a good tailoring of its percentage as well as its particle size in the porcelain composition. The reduction of the flexural strength above 1100 °C for P1 and 1150 °C for P2 indicates that increasing quartz proportion may have increased the maturation temperature and flexural strength.

3.4. Apparent density and water absorption

The water absorption and apparent density of prepared specimens at indicated temperatures is presented in Figure 10.

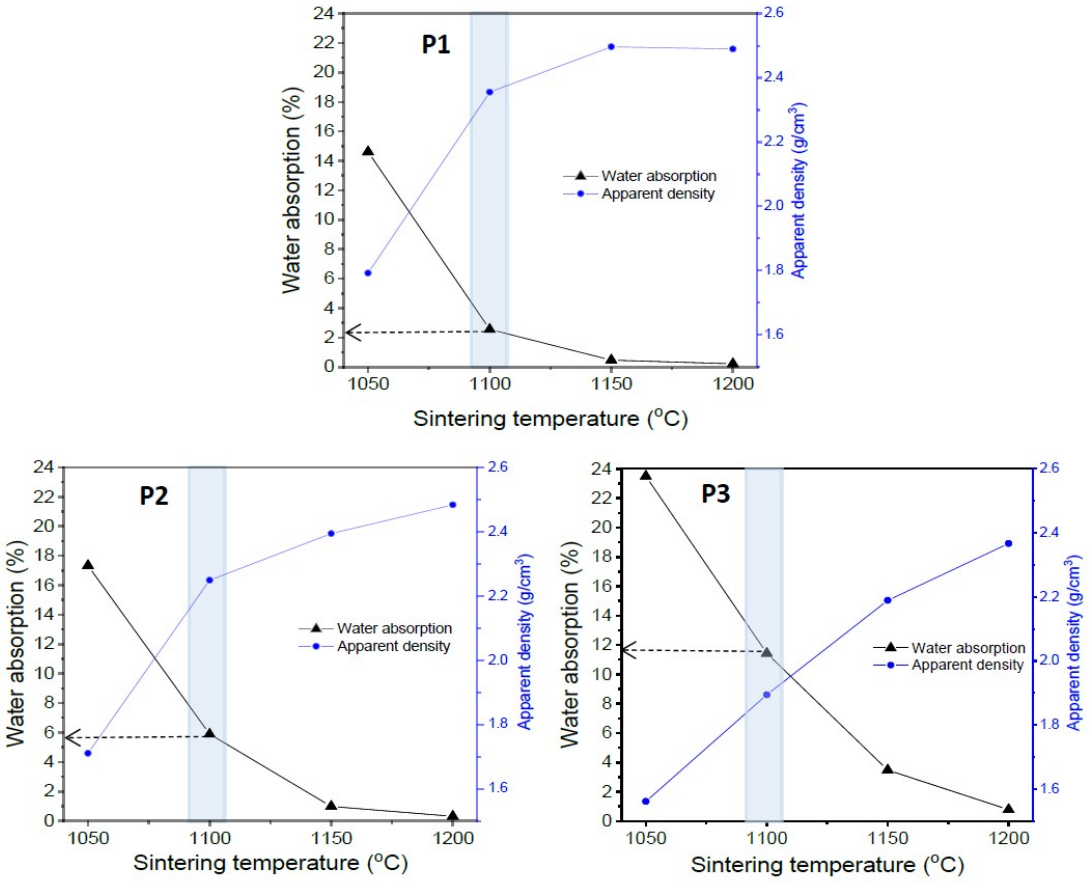

Figure 10: Effect of sintering temperature on water absorption and apparent density of P1(QFS50K50), P2 (QFS41Q9K50) and P3(Q25K50F25)

The trend observed is a decrease of water absorption and an increase of the apparent density with the increase of the sintering temperature. However, the values of water absorption and apparent

density are varying in different ways for each composition, as highlighted for specimens sintered at 1100°C. The composition P1 containing 50 wt% QFS and 50 wt% kaolin had the lowest water absorption, likely ascribed to the good fluxing effect of QFS which is in line with the SEM and compressive strength results. The substitution of 9 wt% of QFS with quartz (i.e. sample P2) slightly increased water absorption and the results of samples containing QFS were comparable to the reference sample which presented slightly higher values of water absorption. At 1200 °C, the water absorption values were about 0.2, 0.6 and 0.8 % for P1, P2 and P3, respectively, meanwhile apparent density values were 2.5 g/cm^3 for P1 and P2 and 2.4 g/cm^3 for P3, values which are comparable to those obtained in some reported studies on porcelain materials (Lima et al., 2018; Owoeye et al., 2018). From these results, it can be deduced that increasing QFS beyond 50 wt% in the mixture could help to increase the extent of sintering and reduce water absorption at 1050 °C, with possible better mechanical performance. In porcelain processing, apparent density are found to present similar behaviour as linear shrinkage (Martín-Márquez et al., 2008), increasing with the increase in the sintering shrinkage. This corroborates with the reduction of water absorption with increasing temperature, as well as the increase in densification with heating temperature observed in microstructural analysis.

3.5. Dilatometry and thermogravimetric analysis

The dilatometry curves of the 3 compositions is presented in Figure 11.

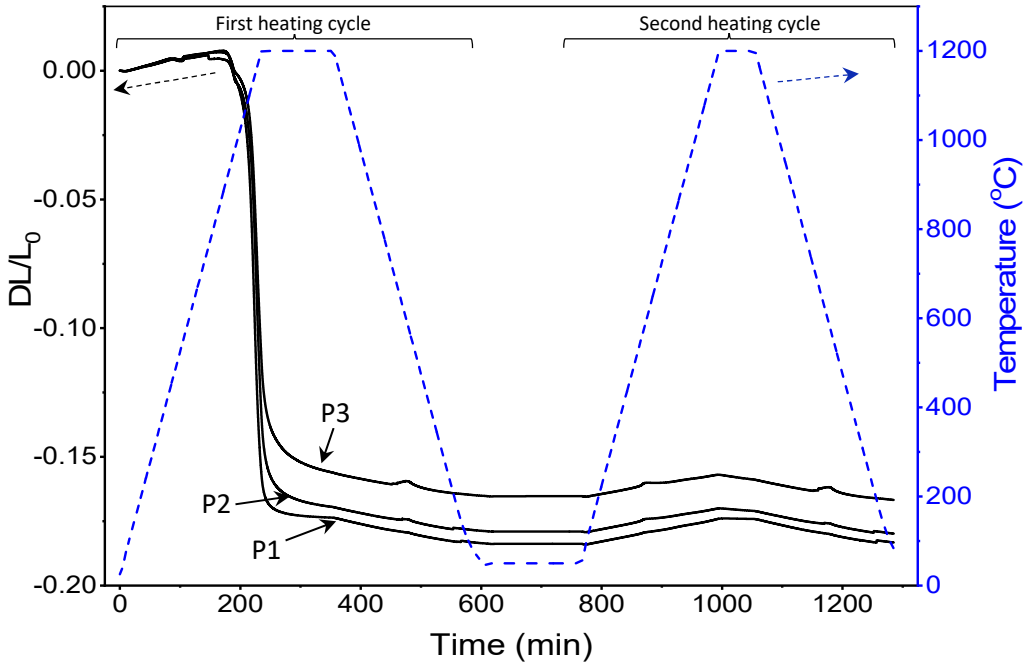

Figure 11: Dilatometry curves of P1(QFS50K50), P2(QFS41Q9K50) and P3 (Q25K50F25)

The three compositions remained relatively stable until about 900 °C, before starting to shrink considerably until 1200 °C. Densification was marked by a sintering shrinkage with a final DL/L0 of 16-18%. During cooling, the change in length was only due to the recovery of thermal expansion, and remained almost linear, with the coefficient of thermal expansion between 500 and 85 °C of 5.6, 6.7 and 7.1×10^{-6} K^{-1} for P1, P2 and P3 respectively. These values are close to some reported values on porcelains (Tarhan et al., 2017). Some defections in the curves were observed around 573 °C in both heating and cooling, due to the remaining quartz in the materials, and were more marked for P2 and P3 containing higher amount of quartz.

The total sintering shrinkage at 1200 °C after the first heating cycle was 18.4, 17.9 and 16.6% for P1, P2 and P3 respectively. These values were close to the reported value of about 20% sintering shrinkage of some porcelain compositions at 1200 °C (Lima et al., 2018).

At 1050 °C, the sintering shrinkages of the three compositions were similar, around 2 %. It is worth reminding that the specimen containing QFS presented a compressive strength of about 40 MPa. The lower value for sintering shrinkage observed at 1050 °C, coupled with the good mechanical properties, is beneficial for the development of structural ceramics from QFS and kaolin around this temperature. The sample P1 prepared with QFS was found to perform very well in densification, suggesting QFS as suitable substitute for the replacement of feldspar and quartz in the production of porcelains and other ceramic materials.

During the second heating cycles, the materials only expended almost linearly until 1200 °C and no additional permanent shrinkage was observed. This dimensional stability suggests a possible use of the materials for some refractory applications up to 1200 °C.

The TG curves of kaolin, QFS and porcelain compositions are presented in Figure 12.

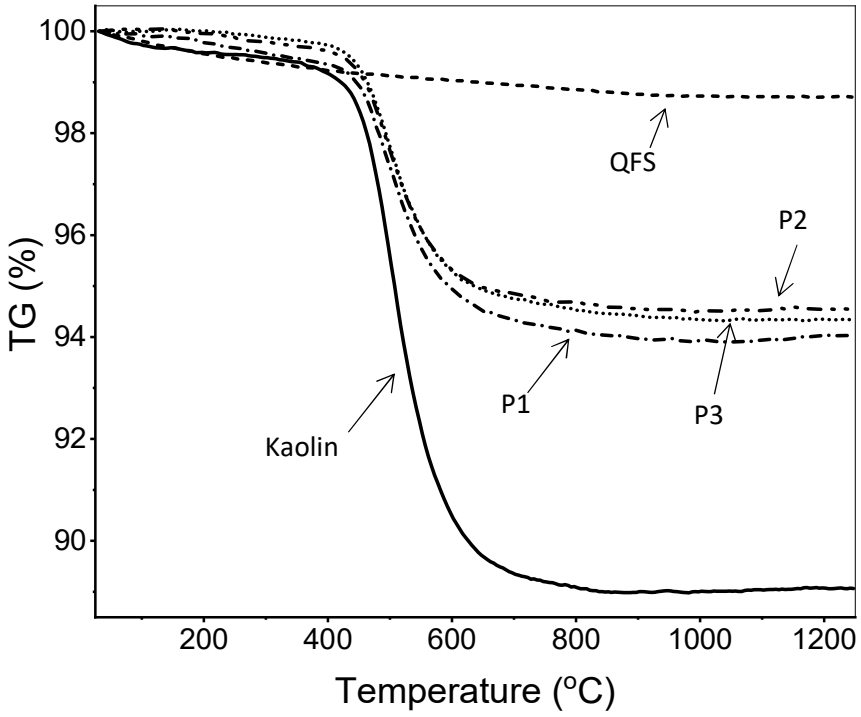

Figure 12: TG curves of kaolin, QFS, P1(QFS50K50), P2(QFS41Q9K50) and P3 (Q25K50F25)

Kaolin was found to present a mass loss of about 11 % at 900 °C and no further mass loss was observed until 1200 °C, while the porcelain compositions presented at 900 °C a mass loss of 5.9, 5.4 and 5.7 % for P1, P2 and P3 respectively; no further variations were observed until 1200 °C. The QFS presented a mass loss of 1.3 % at 1200 °C, ascribed to the loss of residual adsorbed atmospheric water and the dihydroxylation of the traces of muscovite. It is noted that the TG curves of compositions prepared with QFS were comparable to the one of P3, the reference porcelain composition. The values of mass loss of P1, P2 and P3 at 1200 °C are comparable to some reported values on porcelains (Martín-Márquez et al., 2008), further confirming the suitability of QFS as secondary raw materials for porcelain manufacturing.

The visual appearance of the prepared specimens at 1050 and 1200 °C is presented in Figure 13.

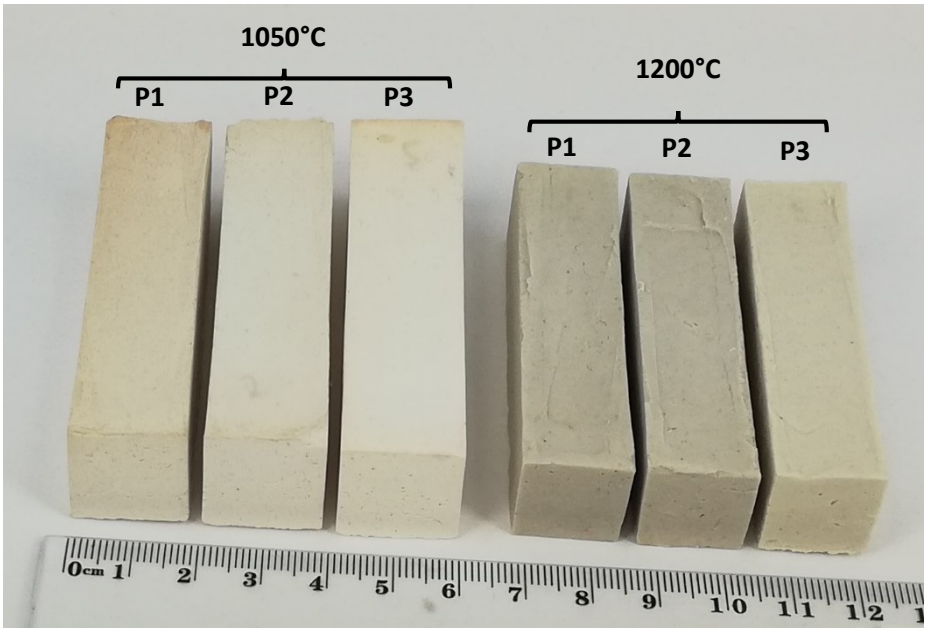

Figure 13: Specimens sintered at 1050 and 1200°C

Colour is often considered for porcelain materials. Colour relies on the purity of materials including kaolin which should contain no or only trace of impurities such as iron and manganese oxides. The kaolin used in this study was not of very high purity grade, containing up to 1.2 wt% Fe_2O_3. This iron impurity has reduced the whiteness of the materials, that presented a grey colour with a

tendency to white. The white tendency was however more marked at 1200 °C for the reference composition (P3), possibly due to the lower content of iron impurity in the commercial feldspar. Hence, QFS is relatively clean, but contains colouring impurities so it could be used without purification in applications where the highest whiteness is not required.

Based on these promising results at 1050 °C, a new set of compositions was designed (S1-2, Table 2) consisting of 80 and 90 wt% QFS, partly substituting kaolin, quartz and feldspar (Table 1).

3.6. Physical properties of compositions S1 and S2

The physical properties of compositions containing 80 and 90 wt% QFS treated at 1050 °C are summarised in Table 3.

Table 3: Physical properties of compositions S1 and S2 treated at 1050 °C

Composition	Compressive strength (MPa)	Flexural strength (MPa)	Water absorption (%)	Apparent density (g/cm^3)
S1 (QFS80K20)	69 ± 5	16.5±2.5	6.8±0.8	2.05±0.05
S2 (QFS90K10)	67 ± 3	17.5±1.5	6.3±0.7	2.07±0.05

The most important engineering quality index for building materials such as bricks is the compressive strength (Taurino et al., 2017). The compressive strength obtained for both S1 and S2 compositions (around 70 MPa) is above the requirement of 17-20 MPa for paving bricks subjected to light traffic, as well as the one of most building materials (Murmu and Patel, 2018; Taurino et al., 2017), suggesting high suitability of the QFS- based ceramics for structural applications. The values of water absorption of S1 and S2 were 6.8 and 6.3 % respectively, well below 15%, satisfying the requirement of the QFS based ceramics for building applications according to ASTM standards C216 (SW).

3.7. Environmental assessment of QFS

The results presented above clearly demonstrate that QFS is a very good candidate for quartz and feldspar substitute in ceramic industry. All felsic mining tailings rich in quartz and felspars could be suitable for mullite based ceramic materials as well. These tailings include molybdenum ore tailings, gold ore tailings and quartz ore tailings (Karhu et al., 2018). However, since the concentration of heavy metals and naturally hazardous elements may be higher in some tailings than in the parent ore (Krivenko et al., 2017), their content need to be measured to ensure its environmentally friendly suitability for the targeted use. The total concentration of heavy metals in QFS, determined by ICP-OES method and compared with the threshold and guideline values of some common harmful substances in soil as total concentration per dry matter is presented in Table 4.

Table 4. Concentration of metals in QFS and comparison with Finnish regulation

Total concentrations of metal in QFS [mg/Kg]		Finnish Government Decree on the Assessment of Soil Contamination and Remediation Needs 214/2007			
Element	**Concentration**	**Natural concentration [mg/Kg]**	**Threshold value [mg/Kg]**	**Lower guideline value [mg/Kg]**	**Higher guide line value [mg/Kg]**
As	<5*	0.1-25	5	50	100
Cd	<1*	0.01-0.15	1	10	20
Co	<1*	1-30	20	100	250
Cr	2.12	6-170	100	200	300
Cu	1.09	5-110	100	150	200
Ni	<2*	3-100	50	100	150
Pb	<5*	0.1-5	60	200	750
Sb	<20*	0.01-0.2	2	10	50
V	1.27	10-115	100	150	250
Zn	3.51	8-110	200	250	400
Hg	-	<0.005-0.05	0.5	2	5

*Under the detection limit

From information in Table 4, it can be deduced that QFS is an environmentally friendly material and can be used as feedstock material in ceramic industry to fulfil the concept of zero waste and circular economy, with related advantage on environment and sustainability. Another economic advantage associated to the use of these tailings is their powder state (d50 of 171 µm for received QFS), which can allow savings from grinding energy. Therefore, the results obtained here are of great interest for both sustainability and economy and could also help to valorise other type of tailings in the manufacturing of ceramic materials.

4. Conclusions

The concept of zero waste is gaining more and more attention, driven by the need for more sustainability and materials efficiency. The present study demonstrated that Quartz Feldspar Sand tailings (QFS) from spodumene processing during lithium chemical production can be used as feedstock materials for the development of porcelain and structural materials, with an advantage for the mitigation of the depletion of feldspar resources. The properties of the porcelain materials prepared with QFS were comparable to those of the reference porcelain composition prepared under the same conditions and some reported values in the literature. Furthermore, QFS was found to be environmentally friendly and suitable for the development of structural ceramics at temperature around 1050 °C. Densification at 1050- 1200 °C resulted from the increase of the amorphous content in the prepared compositions, with the disappearance of feldspar reflections and the increase of mullite phase. Water absorption values ranged from 24% at 1050 °C to below 1% at 1200 °C, with lower values obtained with specimens prepared with QFS. The compressive and flexural strength were respectively in the range 20-95 MPa and 5-30 MPa. The dilatometry analysis showed a comparable shrinkage curves within 25-1200 °C, with a total sintering shrinkage of 16-18 % after the first heating cycle at 1200 ºC. During the second heating cycle at 1200 ºC, the materials

remained relatively stable, with no sintering shrinkage and coefficients of thermal expansion between 85 and 500 ºC of 5.6, 6.7 and 7.1 $\times 10^{-6}$ K^{-1} for P1(QFS50K50), P2(QFS41Q9K50) and P3(Q25K50F25) respectively, comparable to that of some porcelains. Compositions containing QFS showed promising results in comparison to the reference composition (P3). The QFS was found highly suitable to produce porcelains when the highest whiteness is not required. Aside from that, the fact these tailings are in the powder form can allow some savings from grinding energy. The overall results are of great interest for a sustainable use of resources and the valorisation of QFS and similar tailings for porcelain and structural materials, complying with the concept of zero waste and circular economy.

Acknowledgements

This work was performed under the framework of the "GEOBOT" project, supported by the European Regional Development Fund (ERDF), Pohjois-Pohjanmaa Council of Oulu Region and Vipuvoimaa EU:lta 2014-2020 and companies Boliden Harjavalta Oy, Keliber Oy and Saint-Gobain Finland Oy.

References

Ahmed Dabwan, H.A., Rubaiah Bt. Che Jaafar, F., 2018. Towards zero emission concepts: High content colloidal silica removal by using paper sludge ash as inorganic coagulant. Materials Today: Proceedings 5, 21559–21565. https://doi.org/10.1016/j.matpr.2018.07.004

Al-Fakih, A., Mohammed, B.S., Liew, M.S., Nikbakht, E., 2019. Incorporation of waste materials in the manufacture of masonry bricks: An update review. Journal of Building Engineering 21, 37–54. https://doi.org/10.1016/j.jobe.2018.09.023

Aylmore, M.G., Merigot, K., Rickard, W.D.A., Evans, N.J., McDonald, B.J., Catovic, E., Spitalny, P., 2018. Assessment of a spodumene ore by advanced analytical and mass spectrometry techniques to determine its amenability to processing for the extraction of lithium. Minerals Engineering 119, 137–148. https://doi.org/10.1016/j.mineng.2018.01.010

Boltakova, N.V., Faseeva, G.R., Kabirov, R.R., Nafikov, R.M., Zakharov, Y.A., 2017. Utilization of inorganic industrial wastes in producing construction ceramics. Review of Russian experience for the years 2000–2015. Waste Management 60, 230–246. https://doi.org/10.1016/j.wasman.2016.11.008

Burlakovs, J., Jani, Y., Kriipsalu, M., Vincevica-Gaile, Z., Kaczala, F., Celma, G., Ozola, R., Rozina, L., Rudovica, V., Hogland, M., Viksna, A., Pehme, K.-M., Hogland, W., Klavins, M., 2018. On the way to 'zero waste' management: Recovery potential of elements, including rare earth elements, from fine

fraction of waste. Journal of Cleaner Production 186, 81–90. https://doi.org/10.1016/j.jclepro.2018.03.102
Carty, W.M., Senapati, U., n.d. Porcelain—Raw Materials, Processing, Phase Evolution, and Mechanical Behavior. Journal of the American Ceramic Society 81, 3–20. https://doi.org/10.1111/j.1151-2916.1998.tb02290.x
Dalkılıç, N., Nabikoğlu, A., 2017. Traditional manufacturing of clay brick used in the historical buildings of Diyarbakir (Turkey). Frontiers of Architectural Research 6, 346–359. https://doi.org/10.1016/j.foar.2017.06.003
Danezan, A., Delaizir, G., Tessier-Doyen, N., Gasgnier, G., Gaillard, J.M., Duport, P., Nait-Ali, B., 2018. Selective laser sintering of porcelain. Journal of the European Ceramic Society 38, 769–775. https://doi.org/10.1016/j.jeurceramsoc.2017.09.034
Esmaeilian, B., Wang, B., Lewis, K., Duarte, F., Ratti, C., Behdad, S., 2018. The future of waste management in smart and sustainable cities: A review and concept paper. Waste Management 81, 177–195. https://doi.org/10.1016/j.wasman.2018.09.047
Fernandes, H.R., Ferreira, J.M.F., 2007. Recycling of chromium-rich leather ashes in porcelain tiles production. Journal of the European Ceramic Society 27, 4657–4663. https://doi.org/10.1016/j.jeurceramsoc.2007.03.037
Gouvêa, D., Tisse Kaneko, T., Kahn, H., de Souza Conceição, E., Antoniassi, J.L., 2015. Using bone ash as an additive in porcelain sintering. Ceramics International 41, 487–496. https://doi.org/10.1016/j.ceramint.2014.08.096
Guan, Y., Huang, G., Liu, L., Huang, C.Z., Zhai, M., 2018. Ecological network analysis for an industrial solid waste metabolism system. Environmental Pollution. https://doi.org/10.1016/j.envpol.2018.10.052
Güngör, F., Ay, N., 2018. The effect of particle size of body components on the processing parameters of semi transparent porcelain. Ceramics International 44, 10611–10620. https://doi.org/10.1016/j.ceramint.2018.03.086
Karhu, M., Lagerbom, J., Solismaa, S., Honkanen, M., Ismailov, A., Räisänen, M.-L., Huttunen-Saarivirta, E., Levänen, E., Kivikytö-Reponen, P., 2018. Mining tailings as raw materials for reaction-sintered aluminosilicate ceramics: Effect of mineralogical composition on microstructure and properties. Ceramics International. https://doi.org/10.1016/j.ceramint.2018.11.180
Keliber, 2018. Keliber Oy LITHIUM PROJECT Definitive Feasibility Study – Executive Summary, June 14, 2018.
Kitouni, S., Harabi, A., 2011. Sintering and mechanical properties of porcelains prepared from algerian raw materials. CerÃ¢mica 57, 453–460.
Kizinievič, O., Kizinievič, V., Pundiene, I., Molotokas, D., 2018. Eco-friendly fired clay brick manufactured with agricultural solid waste. Archives of Civil and Mechanical Engineering 18, 1156–1165. https://doi.org/10.1016/j.acme.2018.03.003
Korhonen, J., Honkasalo, A., Seppälä, J., 2018. Circular Economy: The Concept and its Limitations. Ecological Economics 143, 37–46. https://doi.org/10.1016/j.ecolecon.2017.06.041
Krivenko, P., Kovalchuk, O., Pasko, A., Croymans, T., Hult, M., Lutter, G., Vandevenne, N., Schreurs, S., Schroeyers, W., 2017. Development of alkali activated cements and concrete mixture design with high volumes of red mud. Construction and Building Materials 151, 819–826. https://doi.org/10.1016/j.conbuildmat.2017.06.031
Kuang, G., Liu, Y., Li, H., Xing, S., Li, F., Guo, H., 2018. Extraction of lithium from β-spodumene using sodium sulfate solution. Hydrometallurgy 177, 49–56. https://doi.org/10.1016/j.hydromet.2018.02.015
Kulkarni, V.V., Golder, A.K., Ghosh, P.K., 2019. Production of composite clay bricks: A value-added solution to hazardous sludge through effective heavy metal fixation. Construction and Building Materials 201, 391–400. https://doi.org/10.1016/j.conbuildmat.2018.12.187
Lassinantti Gualtieri, M., Mugoni, C., Guandalini, S., Cattini, A., Mazzini, D., Alboni, C., Siligardi, C., 2018. Glass recycling in the production of low-temperature stoneware tiles. Journal of Cleaner Production 197, 1531–1539. https://doi.org/10.1016/j.jclepro.2018.06.264
Lemougna, P.N., MacKenzie, K.J.D., Melo, U.F.C., 2011. Synthesis and thermal properties of inorganic polymers (geopolymers) for structural and refractory applications from volcanic ash. Ceramics International 37, 3011–3018. https://doi.org/10.1016/j.ceramint.2011.05.002

Lerdprom, W., Chinnam, R.K., Jayaseelan, D.D., Lee, W.E., 2016. Porcelain production by direct sintering. Journal of the European Ceramic Society 36, 4319–4325. https://doi.org/10.1016/j.jeurceramsoc.2016.07.013

Lima, P., Zocca, A., Acchar, W., Günster, J., 2018. 3D printing of porcelain by layerwise slurry deposition. Journal of the European Ceramic Society 38, 3395–3400. https://doi.org/10.1016/j.jeurceramsoc.2018.03.014

Martin, G., Rentsch, L., Höck, M., Bertau, M., 2017. Lithium market research – global supply, future demand and price development. Energy Storage Materials 6, 171–179. https://doi.org/10.1016/j.ensm.2016.11.004

Martín-Márquez, J., Rincón, J.M., Romero, M., 2010. Effect of microstructure on mechanical properties of porcelain stoneware. Journal of the European Ceramic Society 30, 3063–3069. https://doi.org/10.1016/j.jeurceramsoc.2010.07.015

Martín-Márquez, J., Rincón, J.M., Romero, M., 2008. Effect of firing temperature on sintering of porcelain stoneware tiles. Ceramics International 34, 1867–1873. https://doi.org/10.1016/j.ceramint.2007.06.006

Meshram, P., Pandey, B.D., Mankhand, T.R., 2014. Extraction of lithium from primary and secondary sources by pre-treatment, leaching and separation: A comprehensive review. Hydrometallurgy 150, 192–208. https://doi.org/10.1016/j.hydromet.2014.10.012

Murmu, A.L., Patel, A., 2018. Towards sustainable bricks production: An overview. Construction and Building Materials 165, 112–125. https://doi.org/10.1016/j.conbuildmat.2018.01.038

Owoeye, S.S., Toludare, T.S., Isinkaye, O.E., Kingsley, U., 2018. Influence of waste glasses on the physico-mechanical behavior of porcelain ceramics. Boletín de la Sociedad Española de Cerámica y Vidrio. https://doi.org/10.1016/j.bsecv.2018.07.002

Saeli, M., Tobaldi, D.M., Seabra, M.P., Labrincha, J.A., 2019. Mix design and mechanical performance of geopolymeric binders and mortars using biomass fly ash and alkaline effluent from paper-pulp industry. Journal of Cleaner Production 208, 1188–1197. https://doi.org/10.1016/j.jclepro.2018.10.213

Sokolář, R., Keršnerová, L., Šveda, M., 2017. The effect of different fluxing agents on the sintering of dry pressed porcelain bodies. Journal of Asian Ceramic Societies 5, 290–294. https://doi.org/10.1016/j.jascer.2017.06.001

Soldati, R., Zanelli, C., Guarini, G., Fazio, S., Bignozzi, M.C., Dondi, M., 2018. Characteristics and rheological behaviour of spray-dried powders for porcelain stoneware slabs. Journal of the European Ceramic Society 38, 4118–4126. https://doi.org/10.1016/j.jeurceramsoc.2018.04.042

Swain, B., 2017. Recovery and recycling of lithium: A review. Separation and Purification Technology 172, 388–403. https://doi.org/10.1016/j.seppur.2016.08.031

Swiss Resource Capital AG, 2017. Lithium Report 2017.

Tarhan, B., Tarhan, M., Aydin, T., 2017. Reusing sanitaryware waste products in glazed porcelain tile production. Ceramics International 43, 3107–3112. https://doi.org/10.1016/j.ceramint.2016.11.123

Taurino, R., Karamanov, A., Rosa, R., Karamanova, E., Barbieri, L., Atanasova-Vladimirova, S., Avdeev, G., Leonelli, C., 2017. New ceramic materials from MSWI bottom ash obtained by an innovative microwave-assisted sintering process. Journal of the European Ceramic Society 37, 323–331. https://doi.org/10.1016/j.jeurceramsoc.2016.08.011

Tian, J., Xu, L., Wu, H., Fang, S., Deng, W., Peng, T., Sun, W., Hu, Y., 2018. A novel approach for flotation recovery of spodumene, mica and feldspar from a lithium pegmatite ore. Journal of Cleaner Production 174, 625–633. https://doi.org/10.1016/j.jclepro.2017.10.331

Veleva, V., Bodkin, G., Todorova, S., 2017. The need for better measurement and employee engagement to advance a circular economy: Lessons from Biogen's "zero waste" journey. Journal of Cleaner Production 154, 517–529. https://doi.org/10.1016/j.jclepro.2017.03.177

Wang, Y., Zhu, G., Zhang, L., Lu, D., Wang, L., Zhao, Y., Zheng, H., 2018. Surface dissolution of spodumene and its role in the flotation concentration of a spodumene ore. Minerals Engineering 125, 120–125. https://doi.org/10.1016/j.mineng.2018.06.002

Weishi, L., Guoyuan, L., Ya, X., Qifei, H., 2018. The properties and formation mechanisms of eco-friendly brick building materials fabricated from low-silicon iron ore tailings. Journal of Cleaner Production 204, 685–692. https://doi.org/10.1016/j.jclepro.2018.08.309

Winans, K., Kendall, A., Deng, H., 2017. The history and current applications of the circular economy concept. Renewable and Sustainable Energy Reviews 68, 825–833. https://doi.org/10.1016/j.rser.2016.09.123

Zanelli, C., Dondi, M., Raimondo, M., Beccaluva, L., Vaccaro, C., 2003. Phase transformations during liquid phase sintering of porcelain stoneware tiles: a petrological approach. Presented at the SINTERING 2003, The Materials Research Institute and The Center for Innovative Sintered Products.

Zhang, Y., Hu, Y., Sun, N., Liu, R., Wang, Z., Wang, L., Sun, W., 2018. Systematic review of feldspar beneficiation and its comprehensive application. Minerals Engineering 128, 141–152. https://doi.org/10.1016/j.mineng.2018.08.043